Influence of silver nanoparticles on Er^{3+} up-conversion in CaF_2 precipitated oxyfluoride glass-ceramics

Chenshuo Ma (马辰硕)[1], Jianbei Qiu (邱建备)[1,2], Dacheng Zhou (周大成)[1], Zhengwen Yang (杨正文)[1,2], and Zhiguo Song (宋志国)[1,2]

[1] *College of Materials Science and Engineering, Kunming University of Science and Technology, Kunming 650093, China*

[2] *Key Laboratory of Advanced Materials of Yunnan Province, Kunming 650093, China*

[*] *Corresponding author: qiu@kmust.edu.cn*

Received March 19, 2014; accepted May 20, 2014; posted online July 18, 2014

The influence of silver nanoparticles on Er^{3+} up-conversion in CaF_2 precipitated oxyfluoride glass-ceramics is investigated. After heat-treatments, transmission electron microscopy images show that CaF_2 nano-crystals precipitate in the glass matrix uniformity, and sliver nanoparticles are spread around the CaF_2 nano-crystals simultaneously. Comparing with the samples without Ag doped, high efficiency up-conversion luminescences of Er^{3+} at 540 and 658 nm are distinctly observed in the silver nanoparticles containing glass-ceramics by the 980-nm excitation. Moreover, since the intensity ratio of green and red emissions changes after silver nanoparticles precipitation, the up-conversion mechanism of Er^{3+} is discussed.

OCIS codes: 050.5298, 160.4670.

doi: 10.3788/COL201412.081601.

Rare earth (RE) ions doped phosphors have attracted extensively interest during the past decades due to their special luminescent behaviors and wide applications in fiber lasers, fiber amplifiers, three-dimensional display, optical data storage, medical diagnostics, and high-density memories[1−4]. However, the up-conversion luminescence efficiency of RE ions is too low to be widely used in practice. Now there is a general consensus that two methods can improve the efficiency of up-conversion luminescence[5]: (1) doped RE ions are confined in crystalline environments with low phonon energy, and the excited state lifetimes and optical absorption cross-sections of RE ions become large compared to those in vitreous environments; (2) since non-radiative energy transfer from a RE ion behaving as an energy donor to one behaving as an energy acceptor, the up-conversion luminescence intensity therefore are enhanced by co-doping other kinds of RE ions.

Recently, it is found that noble metal such as Ag and Au doped glasses begins entering into the field of improving the quantum yield of up-conversion luminescence. Indeed, the precipitated metal nanoparticles (NPs) played crucial roles in the luminescence enhancement due to the surface plasmon resonance (SPR) effect[6,7]. When the excitation wavelength matches well with approximate from the SPR wavelength λ_{sp}, the luminescence enhancement or quenching may occur meanwhile[8]. The luminescence of RE ions can be enhanced by the SPR effect of the metal NPs[9,10] and then the radiative transition is encouraged in the low phonon energy environment. In previous work, the Ag NPs were prepared by silver ion-exchange[11], in this case, Ag^+ and various silver aggregates such as Ag_2^+, Ag_3^+, Ag dimers etc. may coexist in the glass matrix, and they may affect the stability of silver dimers, finally, silver NPs will precipitated from glass matrix due to silver aggregates polymerization at high temperatures.

Though the work about metallic NPs enhanced up-conversion luminescence has been reported[12−14], the influence of metallic NPs on the mechanism of up-conversion luminescence is still ambiguous and need to be discussed further. While in our case, the main purpose of our research is Ag NPs effect on the up-conversion luminescence of RE ions, Ag^+, Ag aggregates, or Ag dimers are transformed to Ag NPs in heat-treatment process, and those are stable in the glass ceramic.

In this letter, the samples were prepared with the following composition (in mol%): $49.5SiO_2$-$19.8Al_2O_3$-$29.7CaF_2$-$1ErF_3$ − xAg_2O (x=0, 0.1, 0.4). About 10 g batch of chemical materials were mixed and melted in a covered alumina crucible at 1 400 °C for about 30 min. Then the glasses were quenched onto a preheated stainless steel mold. The quenched sample was annealed at 550 °C for 4 h and cooled slowly down to the room temperature. Then, the glass samples were cut into a size of 10×10×2 (mm) and the surfaces were polished for optical measurements, named them as 0AG, 0.1AG, and 0.4AG. Then the glass samples were heat treated at 655 °C for 4 h to introduce the transparent glass-ceramics. The corresponding glass-ceramics samples are named as 0AGC, 0.1AGC, and 0.4AGC, respectively, according to their Ag^+ contents.

Differential thermal analysis (DTA, DTA-60AH, SHIMADZU) is performed for the determination of the glass transition temperature (T_g=521 °C), the onset of crystallization temperature (T_x=657 °C), and bulk crystallization temperature (T_c=876 °C) with a heating rate of 10 °C/min. The formation of CaF_2 crystal phases is confirmed by using X-ray diffraction (XRD, Bruker D8-Advance diffractometer), which is carried out by a powder diffractometer method using Cu Kα radiation (λ=0.154 nm). The Ag NPs and the CaF_2 nano-crystals precipitated in the heated samples were observed by the transmission electron microscopy (TEM, JEM-2100). Fluorescence spectra were measured using a spectrophotometer in the wavelength range of 500–750 nm (Spectrophotometer F7000; Hitachi Ltd.).

Figure 1 shows the DTA curves of the sample doped

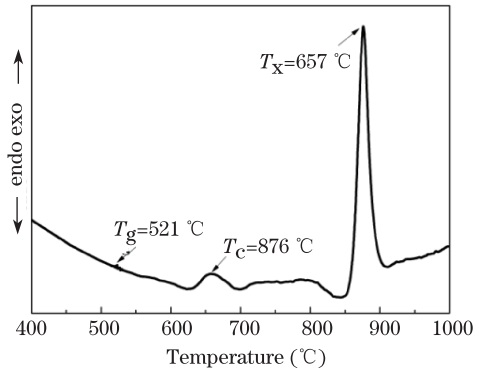

Fig. 1. DTA curve of the $49.5SiO_2$-$19.8Al_2O_3$-$29.7CaF_2$-$1ErF_3$-$0.4Ag_2O$ glass as prepared.

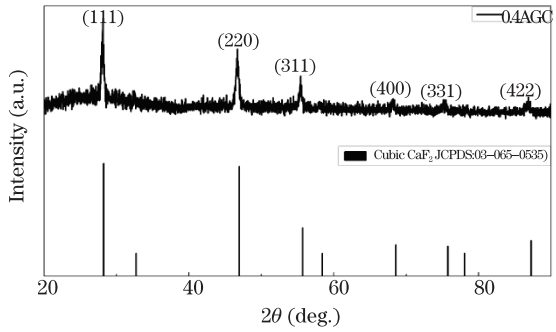

Fig. 2. XRD patterns of the 0.4AGC.

with 1 mol% ErF_3 and 0.4 mol% Ag_2O. As can be seen in Fig. 1, the significant phenomenon that an additional exothermic peak appears between the temperatures of T_g and T_c, means that the microcrystals may be precipitated form the glass matrix when heating at the temperature of T_x. As imagined, the above glass sample is heated at about 657 °C for 4 h and the structure analysis of the glass is investigated in the following work. The XRD patterns of the sample after heat-treatment with the composition of oxyfluoride glasses are displayed in Fig. 2.

For comparison, the reference crystals (CaF_2, JCPDS: 03-065-0535) is illustrated here. It is clearly seen that crystalline peak is well matched at 28.235°, 46.945°, 55.687°, 68.567°, 75.734°, and 87.242° corresponding to the relevant crystal face at (111), (220), (311), (400), (331), and (422) of CaF_2, respectively, revealing that the precipitated microcrystalline are basically pure phase of CaF_2 crystals. Even the peak of Ag cannot be found in the patterns, but we have proved the Ag exists in the sample in latter discussion. Moreover, according to the Scherer equation, the size of the precipitated CaF_2 nano-crystals is calculated as about 23.8 nm, based on the XRD results.

In the case of the presence of microcrystalline, typical Er^{3+} up-conversion luminescence spectra of 0AG, 0AGC, 0.1AGC, and 0.4AGC samples were performed with excitation source at 980 nm.

In Fig. 3, the up-conversion emission bands observed at 540 and 658 nm are due to the transitions of Er^{3+}: $^4S_{3/2} \rightarrow ^4I_{15/2}$ (540 nm) and $^4F_{9/2} \rightarrow ^4I_{15/2}$ (658 nm), respectively. The up-conversion emission intensity (I_{up}) is proportional to the n of the pump power (P) as $I_{up} \propto P_n$ pump, where n is the number of infrared photons required to absorb for emitting one visible photon. The inset in Fig. 3 shows the log-log plots of the emission intensity as a function of excitation power. The values of n for 540 and 658 nm of Er^{3+} ions are close to 2, which indicates that the green and red emissions of Er^{3+} originate from a two-photon populating process. The intensity of the up-conversion luminescence in Ag_2O-doped glass-ceramics was significantly stronger than that without Ag_2O-doped, and the intensity of up-conversion luminescence increased with increase of Ag_2O concentration. According to the results above, it is reasonable to be realized that the increase of the up-conversion luminescence may be related to the SPR of Ag NPs, possibly formed in the glass matrix during the annealing process.

It is difficult to estimate Ag NPs precipitating during heat-treatment by naked eyes, since the glass-ceramics keeps colorless with Ag_2O addition. In the previous reports, it is known that a broad absorption band at around 400±20 nm[15–17] appeared in Ag NPs precipitated glasses, the absorption spectra therefore, are investigated firstly.

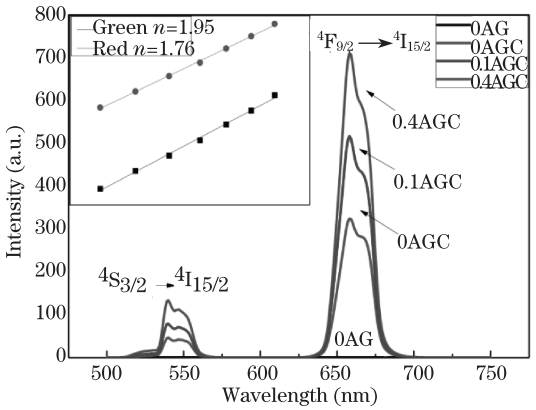

Fig. 3. Up-conversion emission spectra of 0AG, 0AGC, 0.1AGC, and 0.4AGC glasses after heat treatment at 655 °C for 4 h under the 980-nm excitation. Inset shows the log-log plots of the emission intensity as a function of excitation power.

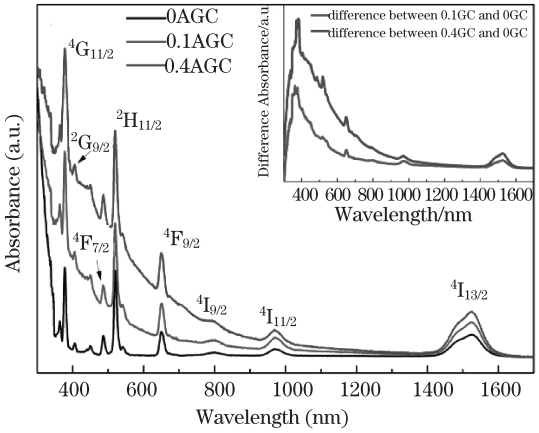

Fig. 4. Absorption spectra of glass-ceramics with $0.4Ag_2O$, $0.1Ag_2O$, and $0Ag_2O$-doped samples annealing at 655 °C for 4 h. The absorption spectra of as-prepared glasses and Ag_2O content glasses.

Figure 4 shows the absorption spectra of Er^{3+}-doped heat treated glasses dependent of Ag contents in the region of 300-1700 nm. For all the samples, eight excited levels are observed, attributed to the electron transitions of Er^{3+} ions. One can see that with increase of Ag_2O concentration, the cross section of RE absorption is apparently increased with a dopant of Ag_2O in the matrix. On the other hand, from the insert in Fig. 4, it is noteworthy that an obvious absorption band is formed at about 400 nm and it increases with increase of Ag_2O doped, and it may be assigned to the small size of sliver NPs. Therefore, it is believed that the sliver NPs precipitated in the CaF_2 nano-crystals containing glass-ceramics, and the Er^{3+} up-conversion luminescence may be enhanced from the light enhancement effect induced by the SPR of Ag NPs.

In order to prove Ag NPs precipitating with CaF_2 nano-crystals during heat-treatment process, TEM measurements were carried out.

As can be seen in Fig. 5(a), in the sample without Ag_2O addition, lots of spherical CaF_2 nano-crystals are precipitated in the glass matrix after heat treatment and distribute homogenously with size of about 20–30 nm which is in good agreement with the size calculated from XRD results. While in Fig. 5(b), 0.4 mol% Ag-doped glass-ceramic sample are interspersed with much of Ag NPs surrounding the CaF_2 nano-crystals and the crystal lattice of the Ag NPs can be easily observed from the inset. Since the size of Ag NPs is just about 5 nm which is much smaller than the CaF_2 nano-crystals, the XRD pattern cannot appeare the peak of Ag with the strong peak of CaF_2.

It is possible that the luminescence enhancement or quenching effect may occur in Ag NPs and RE co-doped glasses. Figure 6 presented the Er^{3+} photoluminescence behavior of the up-conversion luminescence and the infrared emission in Ag NPs precipitated glass-ceramic.

As can be seen in Fig. 6(a), after normalization in the green luminescence at 540 nm, obvious decrease of the red emission at 658 nm is observed with Ag NPs

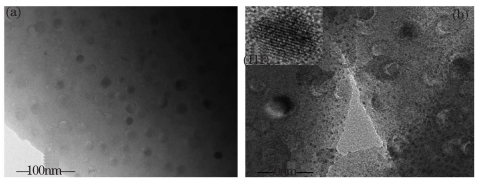

Fig. 5. TEM micrographs of (a) the sample without Ag_2O addition and (b) the Ag_2O containing sample.

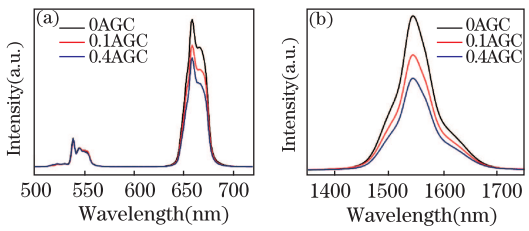

Fig. 6. (a) Ratio of green up-conversion luminescence to red luminescence. (b) The infrared emission spectra of glass-ceramics samples with different Ag_2O contents under the 980-nm excitation.

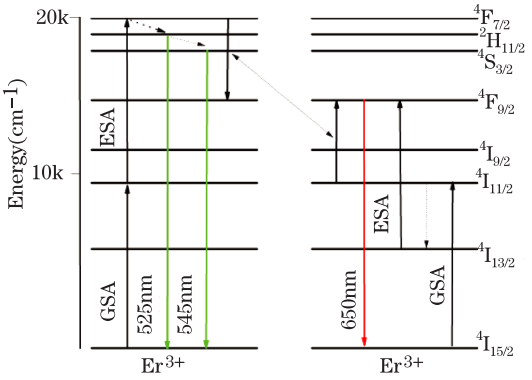

Fig. 7. Up-conversion mechanisms of Er^{3+}-doped glass-ceramics under the 980-nm excitation.

precipitation. This result demonstrated that the efficiencies of the up-conversion luminescences between green and red parts were different, and the SPR effect of the Ag NPs was inclined to participate in the promotion of the electron transition of green emission. On the other hand, as in Fig. 6(b), the Er^{3+} infrared emission at 1540 nm decreased with Ag_2O addition under the 980-nm excitation. The different luminescence variations of same RE ions at different wavelengths implied that distinct interaction mechanism happened in different energy levels of Er^{3+} electron transitions. The observation of both enhancement and quenching effect of Ag NPs was realized in the Er^{3+}-doped glass-ceramic which contained Ag NPs in the matrix. Maybe the different energy level transitions were related to the special SPR wavelength of the Ag NPs formed in our glass matrix.

In fact, it is clarified that molecule-like Ag particles such as dimer, trimers, and tetramers will be generated during Ag NPs formation, a correct assignment of the different enhancement mechanisms, therefore, is very complicated, because the particle can also quench the luminescence of molecules by non-radiative transfer from the excited state to the metal under excitation of plasmon that subsequently decay non-radiatively[18]. To further illuminate this physical process, the mechanism of the up-conversion process is depicted in Fig. 7, and the relationship between up-conversion luminescence intensity and the pumping power is studied.

In this process, Er^{3+} is raised from the $^4I_{15/2}$ ground state to $^4F_{7/2}$ excited state through the ground state absorption (GSA) and excitation state absorption (ESA), and then gets the green luminescence by non-radiative relaxation (NR). At the same time, Er^{3+} is raised from the $^4I_{15/2}$ ground state to $^4I_{11/2}$ excited state through GSA, and gets the red luminescence after NR and ESA. The routs can be described as

$$^4I_{15/2} \xrightarrow{GSA} {}^4I_{11/2} \xrightarrow{ESA} {}^4F_{7/2} \xrightarrow{NR} {}^2H_{11/2}/{}^4S_{3/2} \rightarrow {}^4I_{15/2}(\text{Green luminescence}),$$

$$^4I_{15/2} \xrightarrow{GSA} {}^4I_{11/2} \xrightarrow{NR} {}^4I_{13/2} \xrightarrow{ESA} {}^4F_{9/2} \rightarrow {}^4I_{15/2}(\text{Red luminescence}).$$

Since the absorption cross section of the Er^{3+} increased with Ag NPs precipitation on $^4I_{11/2}$, the efficiency up-conversion becomes higher. Consequently, the green and red up-conversion luminescences obviously increased with Ag_2O addition.

On the other hand, since the absorption cross section of the Er^{3+} decreased with Ag NPs precipitation, the number of electronic layout on the $^4I_{13/2}$ has decreased, so it has fewer electrons can move to the $^4F_{9/2}$ by ESA. Then the enhancement of green up-conversion luminescence becomes higher than the red one.

In conclusion, the transparent oxyfluoride glass-ceramics containing CaF_2 nano-crystals and Ag NPs are successfully prepared. Up-conversion luminescence of Er^{3+} in the glass-ceramics is significantly enhanced with Ag_2O containing in comparison with glass-ceramics without Ag_2O containing, based on the Ag^+ turn to Ag NPs with the process of heat treatment. The up-conversion luminescence intensity in the glass-ceramics increases significantly with the increasing of Ag NPs. All of these phenomena are due to the glass-ceramics with Ag NPs and the NPs have the characteristic of SPR. From this conclusion, we may conjecture that noble metal particles can increase the up-conversion luminescence in glass-ceramics by SPR.

This work was supported by the National Natural Science Foundation of China (Nos. 61265004, 51272097, and 61307111) and the Nature and Science Fund from Yunnan Province Ministry of Education (No. 2011C13211708).

References

1. F. Wang, R. R. Deng, J. Wang, Q. X. Wang, Y. Han, H. M. Zhu, X. Y. Chen, and X. G. Liu, Nat. Mater. **10,** 968 (2011).
2. D. Q. Chen, Y. L. Yu, F. Huang, A. P. Yang, and Y. S. Wang, J. Mater. Chem. **21**, 6186 (2011).
3. D. Yan, Z. Yang, J. Liao, H. Wu, J. Qiu, Z. Song, D. Zhou, Y. Yang, and Z. Ying, Chin. Opt. Lett. **11,** 041602 (2013).
4. W. Li, Q. Zhou, L. Zhang, S. Wang, M. Wang, C. Yu, S. Feng, D. Chen, and L. Hu, Chin. Opt. Lett. **11,** 091601 (2013).
5. J. B. Qiu and A. Makishima, Sci. Technol. Adv. Mater. **5,** 313 (2004).
6. H. Portales, M. Mattarelli, M. Montagna, A. Chiasera, M. Ferrari, A. Martucci, P. Mazzoldi, S. Pelli, and G. C. Righini, J. Non-Cryst Solids. **351,** 1738 (2005).
7. G. Bi, L. Wang, W. Xiong, K. Ueno, H. Misawa, and J. Qiu, Chin. Opt. Lett. **10,** 092401 (2012).
8. L. R. P. Kassab, C. B. de Araújo, R. A. Kobayashi, P. R. de Almeida, and D. M. da Silva, J. Appl. Phys. **102,** 103515 (2007).
9. P. Kumar and V. K. Tripathi, J. Appl. Phys. **106,** 013312 (2009).
10. A. Pillonnet, A. Berthelot, A. Pereira, O. Benamara, S. Derom, G. C. des Francs, and A. -M. Jurdyc, Appl. Phys. Lett. **100,** 153115 (2012).
11. A. Simo, J. Polte, N. Pfander, U. Vainio, F. Emmerling, and K. Rademann, J. Am. Chem. Soc. **134,** 18824 (2012).
12. P. Anger, P. Bharadwaj, and L. Novotny, Phys. Rev. Lett. **96,** 113002 (2006).
13. S. Kühn, U. Håkanson, L. Rogobete, and V. Sandoghdar, Phys. Rev. Lett. **97,** 017402 (2006).
14. H. Lin, D. Q. Chen, Y. L. Yu, R. Zhang, and Y. S. Wang, Appl. Phys. Lett. **103,** 091902 (2013).
15. Y. Wu, X. Shen, S. X. Dai, Y. S. Xu, F. F. Chen, C. G. Lin, T. F. Xu, and Q. H. Nie, J. Phys. Chem. C **115,** 25040 (2011).
16. M. Eichelbaum and K. Rademann, Adv. Funct. Mater. **19,** 2045 (2009).
17. J. A. Jimenez, S. Lysenko, and H. Liu, J. Appl. Phys. **104,** 54313 (2008).
18. S. J. Zhou, M. W. Shao, H. Y. Xu, T. Chen, D. D. D. Ma, and S. T. Lee, J. Appl. Phys. **108,** 034305 (2010).